

© 2020. M. Kaszyńska, S. Skibicki.

This is an open-access article distributed under the terms of the Creative Commons Attribution-NonCommercial-NoDerivatives License (CC BY-NC-ND 4.0, <https://creativecommons.org/licenses/by-nc-nd/4.0/>), which permits use, distribution, and reproduction in any medium, provided that the Article is properly cited, the use is non-commercial, and no modifications or adaptations are made.



EFFECT OF PROTRUDING REBAR FROM CASTING ELEMENT ON TEMPERATURE DEVELOPMENT AND COMPRESSIVE STRENGTH OF MASS CONCRETE

M. KASZYŃSKA¹, S. SKIBICKI²

The influence of rebar, protruding from concrete element during casting, on temperature and strength development was analyzed. Test models of size 50 cm x 50 cm x 50 cm were made with and without protruding rebar. The rebar protruding from the sample simulated the conditions of the hardening of elements such as bridge abutments or pylons, which require technological break. Samples were cast in insulated formworks, to create semi-adiabatic conditions for concrete curing, simulating real conditions of curing of mass structures. The research utilized self-consolidating concrete with two different rapid hardening cements: CEM I 42.5R and CEM I 52.5R, and blastfurnace cement CEM III/A 42.5N. Continuous registration of temperatures in the samples was performed for the first 7 days. Based on the results acquired and compressive strength, the amount and kinetics of the heat given off in the concrete was determined and an evaluation of its strength in conditions simulating actual conditions was performed. The research showed that the difference in temperature between the reinforced and non-reinforced sample was approximately 14.0° C.

Keywords: compressive strength; temperature; self-consolidating concrete; protruding rebar; mass structure

¹ Prof. ZUT, PhD., Eng., West Pomeranian University of Technology, Faculty of Civil Engineering and Architecture, Al. Piastów 17, 70-310 Szczecin, Poland, e-mail: maria.kaszynska@zut.edu.pl

² MSc. Eng. West Pomeranian University of Technology, Faculty of Civil Engineering and Architecture, Al. Piastów 17, 70-310 Szczecin, Poland, e-mail: szymon.skibicki@zut.edu.pl

1. INTRODUCTION

A direct result of exothermic hydration reaction and the hardening of cement binder is a rapid increase in temperature in the concrete mass [1–8]. Temperature development in structures is determined by two opposing phenomena heat emission as a result of the exothermic process of cement hydration and heat exchange between the structure and its surroundings. External conditions vary in day cycles, comprised of factors such as air temperature, wind speed, relative humidity and sunlight [9,10]. The hydration of cement under lab conditions, with constant temperature and humidity, may differ greatly from the conditions at construction sites [11]. These parameters should be taken into consideration in the development of different calculation models for thermal-shrinkage cracking in mass concrete structures. An additional factor affecting the temperature of cured concrete, which is not included in the analysis, is the protruding of rebar from mass elements, such as pylons, during casting.

The process of casting mass pylons is divided into certain stages, often forcing necessary breaks. Rebar prepared for other layers of concrete can protrude from cast elements of pylons. Very often this is ignored in computational analysis of hydration heat [12–15]. Heat escaping through rebar is not included, even though the thermal conductivity of steel is 16 times higher than that of concrete. This issue can additionally occur in heavily reinforced elements, where self-consolidating concretes are necessary [16,17].

Problems connected with self-heating of concretes are particularly important in case of massive concrete structures, in which thermal stresses caused by hydration can be higher than the strength of early age concrete, leading to cracking already in construction stage. The measurements of the self-heating temperature of concrete carried out during construction of structures of this type indicate that inside concrete blocks exist adiabatic curing conditions. According to the definition provided by the American Concrete Institute (2000) [18], a massive element is “any volume of concrete with dimensions large enough to require that measures be taken to cope with generation of heat from hydration of the cement and attendant volume change, to minimize cracking”. However, this definition does not specify any dimensions of said element. Gaida and Vangeem M. (2002) [19], categorize a massive block as being 90 x 90 x 90 cm, in the case of CEM III cement. In other studies, such as those of Ju-Hyung et al. (2014) [20] or Xinghong et al. (2015) [21], the sample sizes are even larger. A similar simulation of a massive construction was undertaken by Silva et al. (2013) [22], who utilised a 24 x 24 x 24 cm block insulated with 10 cm thick extruded polystyrene. They compared the results of this small sample with a massive 1 m³ block and also a 1050 m³ concrete block, with the

results showing that the small sample, isolated as per the researchers' directions, mirrored a massive construction accurately. Nagaratnam et al. (2016) [23] have also demonstrated the possibility of simulating semi-adiabatic conditions using small samples, utilizing a 30 x 30 x 30 cm sample insulated with 5 cm Styrofoam and 2.5 cm glass wool. Similar cases can be found in Abdul Awal and Shehu (2013) [24] as well as Jones and McCarthy (2006) [25]. All of the studies mentioned present a method for mirroring semi-adiabatic or adiabatic conditions pervasive in massive structures, utilizing small samples.

In view of this, the assessment and analysis of cement hydration heat in concrete and its compressive strength were carried out in own investigations in semi-adiabatic conditions. This gave upper assessment of values of heat emitted in concrete.

This article presents the results of tests and analysis of temperature development in non-reinforced concrete blocks and reinforced concrete blocks with protruding rebar and with its influence on the early age strength of cured concrete. The influence of the protruding rebar from the concrete element on the reduction of the concrete hardening temperature was analyzed.

The purpose of the research is to determine the relationship of the amount and kinetics of heat generated and the early-age compressive strength of self-consolidating concretes cured in massive structures. The study is focused on applications in bridge engineering.

2. MATERIALS AND EXPERIMENTAL PROCEDURE

INSTRUCTIONS

2.1. MATERIALS

The tests were performed on three self-consolidating concrete mixtures (M1, M2, M3) made with Portland cement CEM I 52.5R, CEM III/A 42.5 N and CEM I 52.5 R (European Standard EN 197-1:2000 [26]), fly ash, superplasticizer, natural sand 0-2 mm and natural aggregates 2-8 mm. The notation of concrete mixes is listed in Table 1.

Table 1. Concrete mix composition

Mix	M1	M2	M3
types of cement	CEM I 52.5R	CEM III/A 42.5N	CEM I 42.5R
cement [kg/m ³]	450	450	450
fly ash [kg/m ³]	110	110	110
superplasticizer [kg/m ³]	11	11	11
water [kg/m ³]	155	155	155
aggregate 0-2 mm [kg/m ³]	623	623	623
aggregate 2-8 mm [kg/m ³]	1072	1072	1072

The composition of cements and fly ash used in experiments are given respectively in Table 2 and Table 3.

Table 2. Composition of cements used in experiments

chemical compounds	CEM I 42.5R	CEM I 52.5R	CEM III/A 42.5N
SiO ₂	19.75	19.7	30.01
Al ₂ O ₃	4.82	4.93	6.21
Fe ₂ O ₃	2.64	2.54	1.99
CaO	64.34	64.23	53.75
MgO	1.4	1.32	2.67
SO ₃	2.91	2.91	2.59
Na ₂ O	0.14	0.12	0.37
K ₂ O	0.76	0.76	0.64
Cl	0.08	0.07	0.08
Na ₂ O _{eq}	0.69	0.63	0.79

Table 3. Composition of fly ash used in experiments

Chemical composition of fly ash [%]	
SiO ₂	54.0
Fe ₂ O ₃	7.3
Al ₂ O ₃	28.4
CaO (complete)	3.1
CaO (free)	0.4
MgO	2.4
SO ₃	0.4
K ₂ O	2.9
Na ₂ O	1.1
ions Cl	0.010

2.2. EXPERIMENTAL PROCEDURE

To quantify heat transfer, a series of tests was performed on specially prepared concrete blocks. Specimens (50 cm x 50 cm x 50 cm) were prepared in a insulated formwork. Two types of samples for each mixtures (M1, M2, M3) were prepared – one without (C) and one with protruding rebar (R). Ribbed steel bars reinforcement grade B500A ($f_{yk} = 500$ MPa, class A according to EN 1992-1-1 (appendix C) [27] and EN 10080 [28]) was used in tests. The ambient temperature in the laboratory was approximately 18-20°C and relative humidity of RH = 55% ($\pm 5\%$).

Rebar used in the samples had a diameter of 2 cm and a length of 80 cm. The ends of the rebar were 20 cm above the bottom of the formwork, protruding 33 cm beyond the top insulation. In each of the reinforced samples, 36 rebar were evenly distributed, constituting a degree of reinforcement of 4.5% (accordingly to EN 1992-1-1 [27] recommended degree of reinforcement value outside lap locations

is 4 %. The study assumed degree of reinforcement of 4.5% due to available diameters of bars and the possibility of their even distribution in cross-section)

The cross section of the sample with protruding rebar are shown in Figure 1.

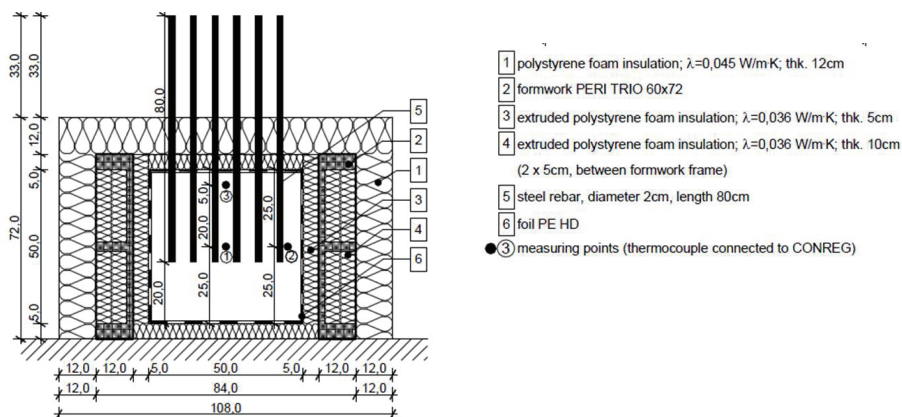


Fig. 1. Reinforced concrete sample (with protruding rebar) – cross section (all dimensions are in cm)

Temperature was measured during curing of the concrete using a type T thermocouple sunken in the concrete mix. The thermocouple was bonded to the rebar in the reinforced samples. In the non-reinforced samples, the thermocouple was placed inside the concrete with a special rod, which was isolated to protect heat loss. The temperature was measured continuously for 7 days in 5 minute intervals with ConReg 706 apparatus.

Both samples of each concrete mix were cast at the same time. The thermocouple was put inside the formwork before casting and was connected to the measuring equipment. The temperature inside the sample was measured at three points: in the middle of the sample (point 1), 5 cm from the side surface (point 2) and 5 cm below the top surface (point 3). The placement and notification of measurement points is shown in Figure 2.

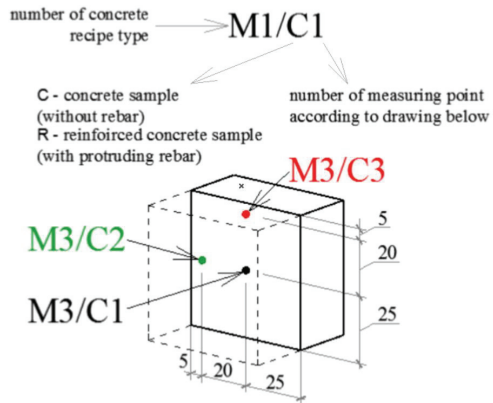


Fig. 2. Location of the measurement points inside sample (all dimensions are in cm)

Figure 3 (a) presents samples inside the formwork filled with extruded polystyrene foam insulation after remove the final top layer of insulation, after testing. Figure 3 (b) presents samples without formwork and insulation after tests.



(a)



(b)

Fig. 3. Samples after tests

Compressive strength of concrete was tested on 15 cm x 15 cm x 15 cm cubes stored in climatic chamber at temperature controlled by the temperature of the 50 cm x 50 cm x 50 cm specimens (without rebar (R) and with protruding rebar (C)). To control the temperature thermocouples form point C1 and R1 was used. The compressive strength was tested after 10, 24, 48, 72, 120, 168 and 672 hours. Schematic diagram of the test stand is shown in Fig. 4.

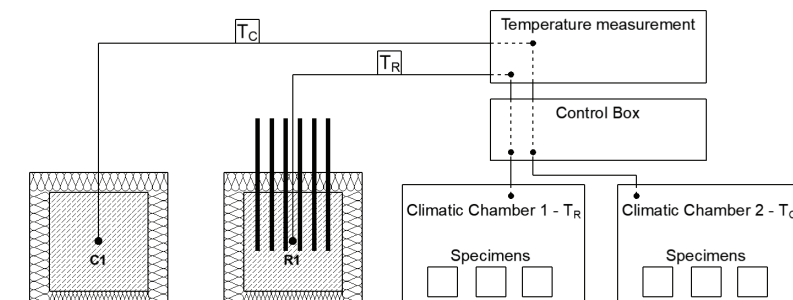


Fig. 4. Schematic diagram of the test stand under semi adiabatic conditions

3. RESULTS

3.1. WORKABILITY PROPERTIES

The concrete's workability properties was measured in a standard tests: Slump-flow Test (EN 206 [29], EN 12350-8 [30]) and Viscosity class test (EN 206 [29], EN 12350-8 [30]). The segregation resistance being evaluated visually (Visual Segregation Index - VSI). Table 4 shows the results of a standard consistency test and concrete mix stability. The results proved that prepared concretes can be classified as self-consolidating concretes.

Table 4. Workability properties of concrete

Concrete	M1	M2	M3
Slump-Flow [mm]	770	840	700
Slump-Flow class	SF3	SF3	SF2
T_{500} [s]	6.5	4.6	5.7
Viscosity class	VS2	VS2	VS2
VSI	0	0	0

3.2. CONCRETE TEMPERATURE MEASUREMENTS

Temperature measurements of the concrete were started immediately after it was cast. Table 5 shows the maximum temperatures in each measurement point, of both non-reinforced (C) and reinforced (R) samples. Coefficient of variation (CoV) of temperature measurements was 0.44% – 3.41% (for 3 specimens).

Table 5. Maximum temperature in concrete samples, T_{max} [°C]

Concrete	C 1		R 1		C 2		R 2		C 3		R 3	
	T_{max} [°]	CoV [%]										
M1	74.9	1.51%	62.3	3.16%	74.3	0.82%	62.1	2.27%	74.5	0.74%	61.1	1.89%
M2	55.3	0.59%	46.0	1.84%	55.5	0.53%	44.2	2.02%	54.3	0.52%	41.9	1.38%
M3	64.9	0.89%	57.9	1.80%	64.2	0.54%	55.9	1.78%	60.9	1.14%	50.9	2.23%

Figures 5 to 7 show the mean temperatures registered in three measurement points in both reinforced and non-reinforced samples of all tested concretes.

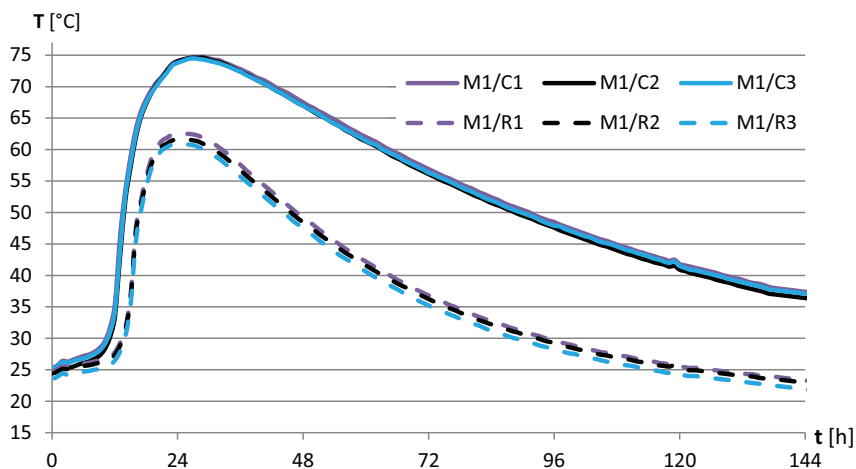


Fig. 5. Results of the temperature measurement in concrete M1

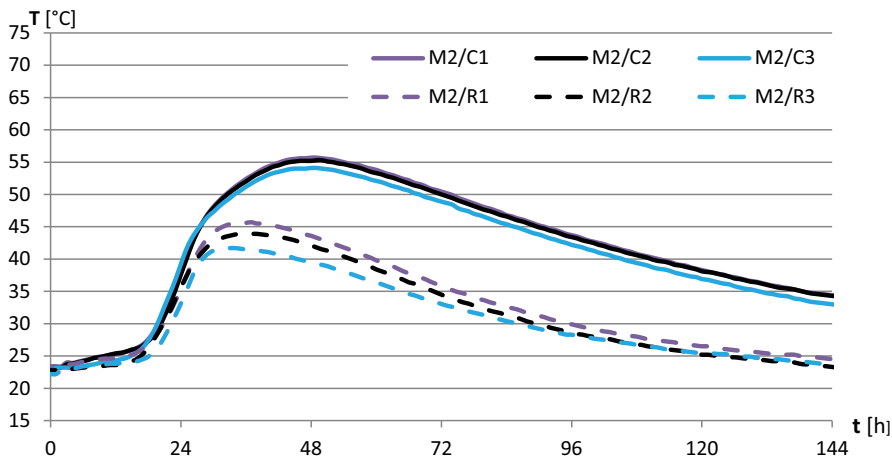


Fig. 6. Results of the temperature measurement in concrete M2

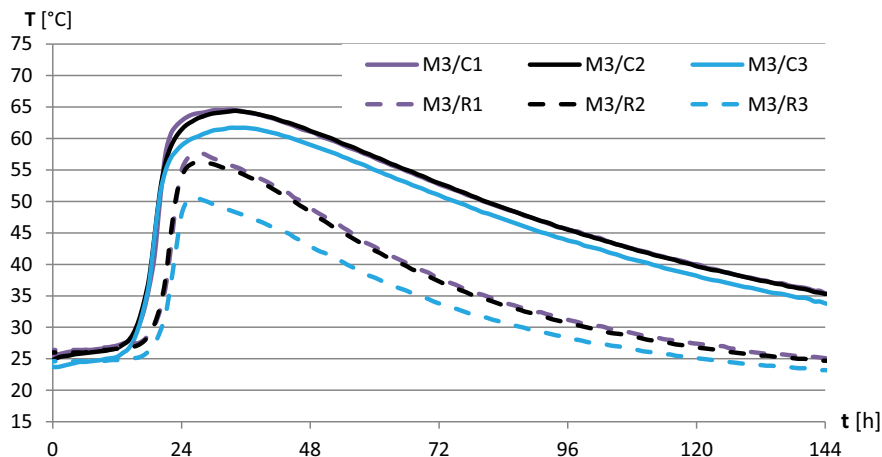


Fig. 7. Results of the temperature measurement in concrete M3

Table 6 shows the time between casting of the mix and the moment when the concrete inside sample reached the maximum temperature.

Table 6. Time after concrete reached maximum temperature [hours]

Concrete	M1	M2	M3
Non-reinforced samples	27	48	33
Reinforced samples	24	37	21

As expected, the highest temperature was measured in concrete with CEM I 52.5 R, followed by concrete with CEM I 42.5R and lastly CEM III/A 42.5N. In non-reinforced concrete, the highest amount of heat emitted was observed for concrete with CEM I 52.5R after 27 hours, with CEM I 42.5R after 33 hours and with CEM III/A 42.5N after 48 hours.

The peaks of the highest temperature for samples with the protruded rebar were as follows: mix M1 after 24 hours, mix M2 after 37 hours and mix M3 after 21 hours. These results are the effect of higher heat escape through the protruded rebar. The effect is magnified by the higher thermal conductivity of rebar compared to concrete and insulation. The difference in time to reach peak temperature, for reinforced and non-reinforced samples, varied from 3 to 12 hours.

During the first hours there is a short period of slow increase, afterwards the temperature spikes rapidly, especially in concretes with CEM I 42.5R and CEM I 52.5R. After reaching the maximum, the temperature starts to drop. The gradients, according to Fourier's law, are higher, when the temperature gradient between the sample and surroundings is higher. The reinforced samples show a similar trend, though in this case the temperature decreased more slowly.

Figure 8 shows a comparison of temperature in the middle point of both reinforced and non-reinforced concrete samples.

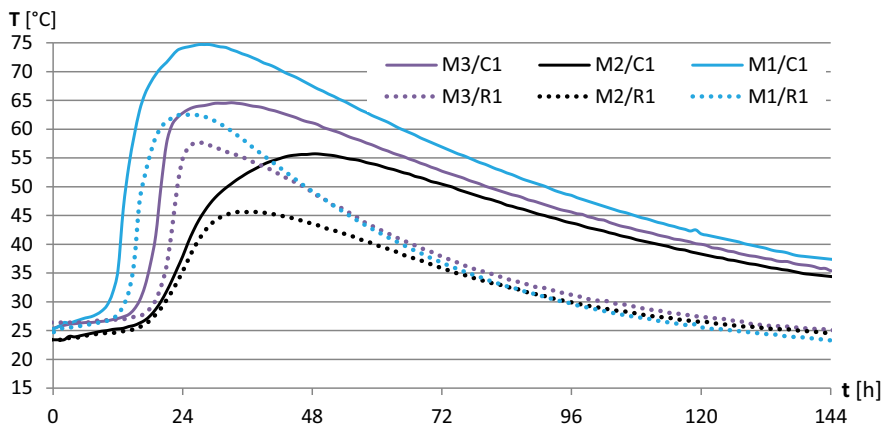


Fig. 8. Temperature inside concrete samples (point 1)

Table 7 shows the self-heating of the self-consolidating concretes ($\Delta T_{max} = T_{max} - T_o$). The test shows that the highest self-heating of concrete $\Delta T_{max} = 51.8$ °C, is exhibited by the non-reinforced concrete with cement CEM I 52.5. When cement CEM III 42.5 was used, the self-heating reached a maximum value $\Delta T_{max} = 32.5$ °C (Table 7).

Table 7. Self-heating of concretes

Concrete	ΔT_{max} [°C]					
	C 1	R 1	C2	R 2	C 3	R 3
M1	51.8	39.5	51.6	38.8	51.0	37.0
M2	32.5	22.5	31.8	20.4	30.5	18.3
M3	40.8	33.9	40.9	32.9	38.6	26.8

Table 8 shows maximum temperature differences between non-reinforced and reinforced samples at three measurement points.

Table 8. Maximum temperature differences between reinforced and non-reinforced concrete

Concrete	Temperature differences [°C]		
	Point (1)	Point(2)	Point (3)
M1	12.3	12.8	14.0
M2	10.0	11.4	12.2
M3	6.9	8.0	11.8

Tests showed that the higher the calorific value of cement, the more heat can escape through rebar, resulting in higher temperature differences. The highest difference was observed at measurement point 3, as a result of the test environment and highest possibility of heat escaping from around the thermocouple.

3.3. COMPRESSIVE STRENGTH OF CONCRETES

The compressive strength of the concrete was tested after 10, 24, 48, 72, 120, 168 and 672 hours of curing:

- 1) under laboratory conditions, at a temperature of 20°C – Table 9;
- 2) under semi –adiabatic conditions according to thermocouple C1– Table 10;
- 3) under semi-adiabatic conditions according to thermocouple R1– Table 11.

Table 9,10,11 shows the mean value of the compressive strength for specific curing times (mean value was calculated from 4 specimens) and Coefficient of Variation (CoV).

Table 9. Compressive strength of concrete [MPa] under laboratory conditions (20°C)

Time	M1		M2		M3	
	f_{cm} [MPa]	Cov [%]	f_{cm} [MPa]	Cov [%]	f_{cm} [MPa]	Cov [%]
10	5.1	4.32%	0.5	5.14%	2.00	4.30%
24	30.93	0.63%	2.05	6.72%	11.63	5.05%
48	56.25	1.37%	27.79	3.12%	35.34	2.14%
72	69.87	1.25%	38.70	2.79%	43.98	2.00%
120	78.14	1.79%	49.64	2.97%	59.42	1.75%
168	81.53	1.34%	56.18	3.00%	65.31	1.41%
672	90.90	1.93%	82.10	2.67%	82.60	2.37%

Table 10. Compressive strength of concrete [MPa] under semi - adiabatic conditions (point C1)

Time	M1		M2		M3	
	f_{cm} [MPa]	Cov [%]	f_{cm} [MPa]	Cov [%]	f_{cm} [MPa]	Cov [%]
10	5,28	4,85%	0,61	3,98%	1,80	4,53%
24	33,40	1,55%	2,38	1,93%	12,68	2,60%
48	58,32	2,75%	32,56	2,13%	38,17	1,98%
72	75,43	3,05%	43,56	2,46%	54,98	2,15%
120	87,02	3,34%	53,45	3,90%	68,27	3,18%
168	88,37	2,27%	58,79	3,28%	70,45	0,91%
672	87,56	0,85%	75,88	0,54%	77,85	0,85%

Table 11. Compressive strength of concrete [MPa] under semi-adiabatic conditions (point R1)

Time	M1		M2		M3	
	f_{cm} [MPa]	Cov [%]	f_{cm} [MPa]	Cov [%]	f_{cm} [MPa]	Cov [%]
10	4,85	2,07%	0,60	3,70%	1,68	3,66%
24	30,15	3,38%	2,30	3,90%	11,56	1,25%
48	57,30	1,09%	31,54	1,44%	36,90	3,92%
72	71,50	3,51%	42,01	3,37%	52,12	4,06%
120	82,73	4,05%	52,11	2,14%	65,09	3,99%
168	85,48	3,25%	56,86	0,90%	68,37	3,46%
672	89,66	4,46%	79,62	3,26%	80,82	2,84%

The comparison of compressive strength of concretes in under laboratory and semi-adiabatic conditions is presented on Fig 9.

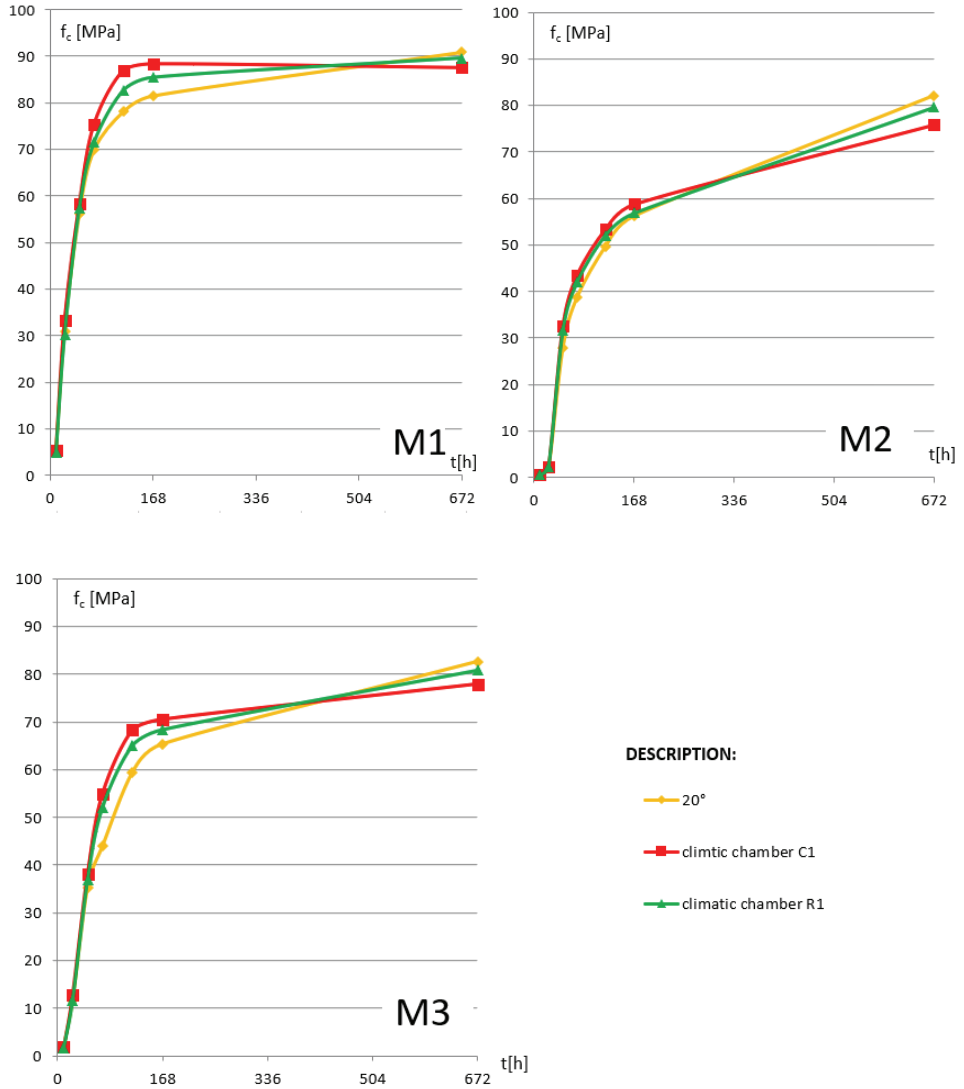


Fig. 9. Compressive strength of concrete under isothermal and adiabatic conditions for concretes M1, M2 and M3

The comparison between compressive strength of concretes under semi-adiabatic conditions for point C1 (central point of specimen without protruding rebars) and point R1 (specimen with protruding rebar) is presented in Table 12. The introduced parameter Δf_{cm} (equation (1)) shows the percentage difference between the compressive strength of concrete sample cured in temperature of C1 ($f_{cm,C1}$) and R1 ($f_{cm,R1}$). The difference between compressive strength of reinforcement and non-reinforcement specimens for mixes M1 and M3 (M1 – with cement CEM I 52.R, M2 – with cement CEM I 42.5R) is very high for early age concrete (about 5 – 15 %) and stabilizes after 48 hours in level about 3 – 5%. For mix M3 (with cement CEM III/A 42.5N) difference between reinforcement and non-reinforcement specimen is about 3-5 % during all maturing period.

$$\Delta f_{cm} = \frac{f_{cm,C1} - f_{cm,R1}}{f_{cm,C1}} [\%] \tag{1}$$

Table 12. The comparison between compressive strength of concretes cured under semi-adiabatic conditions from point C1 and point R1

Time	M1			M2			M3		
t [h]	$f_{cm,C1}$ [MPa] (point C1)	$f_{cm,R1}$ [MPa] (point R1)	Δf_{cm} [%]	$f_{cm,C1}$ [MPa] (point C1)	$f_{cm,R1}$ [MPa] (point R1)	Δf_{cm} [%]	$f_{cm,C1}$ [MPa] (point C1)	$f_{cm,R1}$ [MPa] (point R1)	Δf_{cm} [%]
10	5.28	4.85	8.24	0.61	0.60	1.64	1.80	1.68	6.67
24	33.40	30.15	9.72	2.38	2.30	3.25	12.68	11.56	8.81
48	58.32	57.30	1.74	32.56	31.54	3.13	38.17	36.90	3.32
72	75.43	71.50	5.20	43.56	42.01	3.56	54.98	52.12	5.19
120	87.02	82.73	4.93	53.45	52.11	2.49	68.27	65.09	4.65
168	88.37	85.48	3.27	58.79	56.86	3.27	70.45	68.37	2.96
672	87.56	89.66	-2.40	75.88	79.62	-4.94	77.85	80.82	-3.82

Analysing the influence of concrete hardening temperature on the strength of concrete, it can be seen that there is a so-called cross-over effect, which proves that when concrete matures at high temperatures, its final strength suffers ([31], [32]). However, the size of this effect in this study is insignificant and amount maximum of 4.5% which is close to the coefficient of variation value.

In reference to literature Brooks et al (2007) [32] have observed that, in some cases, heightened temperature can have a beneficial effect on the concrete mix and thus that the final strength is not compromised; indeed that strength may sometimes be enhanced. Opinion regarding the long term strength of concrete under adiabatic conditions is divided. Using 180 cm x 180 cm x 180 cm samples, Yikici and Chen (2015) [33] have noted that temperature causes overestimation in the results of

maturity functions, albeit to only a small degree, as the effects of heightened temperature are short-term. Similar conclusions have been drawn by Lin and Chen (2016) [34,35], who found that, in their mixture, the crossover effect began only at a temperature of 50°C. In their model experiment, using a 120 cm x 120 cm x 120 cm sample, they argued that the influence of high temperature was active for just 10 hours and that this did not change the concrete's final strength. On the other hand, Soutsos et al. (2016) [36] noted a significant effect of temperature on their massive samples and found a significant discrepancy between functions of maturity and reality, particularly in the early stages of maturation. However, in the study by Soutsos et al. (2016) [36], the earliest core samples were taken only after seven days, when the discrepancy between the maturity method and the core sample was up to 15%, but a lack of results prior to the seven day period does not allow one to draw conclusions regarding such discrepancies in the most important maturation period for massive objects. Furthermore, on the basis of the research of Brooks et al. (2007) [32], it can be argued that the crossover effect does not occur in certain mixtures. According to the report of Wade et al. (2006) [37], in mixtures containing 20% fly ash (the type examined in this study), the reduction in strength is just 1%.

3.4. RELATIONSHIP BETWEEN STRENGTH AND HEAT OF HYDRATION

On the basis of the temperature to time curves recorded during the tests, the amounts of heat of hydration of cement in concrete $Q(t)$ and the values of the source function $W(t)=dQ/dt$ (rate of heat evolution) were calculated. Table 13 presents comparison between previously acquired strength and amount, and the kinetics of heat given off in concrete, both in reinforced and non-reinforced samples.

Table 13. Comparison of the compressive strength of concrete M1, M2, M3 at the maximum of dQ/dt

Concrete mix	M1/C1	M1/R1	M2/C1	M2/R1	M3/C1	M3/R1
t [h]	12.00	15.00	23.00	24.00	19.00	21.00
f_{cm} [MPa]	9.78	14.42	3.75	4.65	8.03	9.35
Q [kJ/kg]	253.60	193.38	159.11	110.16	199.75	165.97
W [W/kg]	21.22	19.59	2.86	2.72	14.69	10.20

Figure 10 present functions of concrete strength and kinetics of heat given off in time.

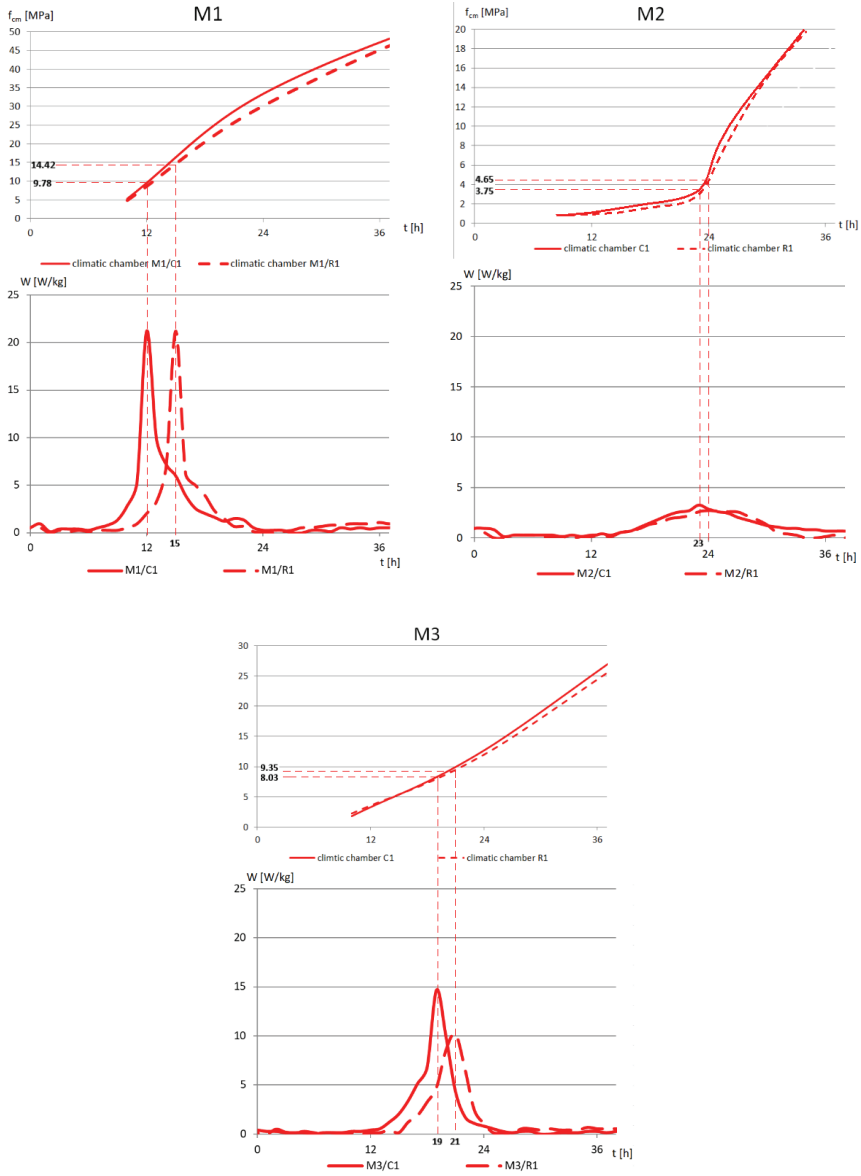


Fig. 10. Compressive strength of concrete M1, M2, M3 at the maximum of dQ/dt

After analysing the following data, it can be stated that the rebar impacts on the translation of the maxima of source function (dQ/dt) by 2-4 h. Higher differences occur in concretes with high calorific cements, which is consistent with Fourier's law.

The compressive strength of reinforced samples M1 and M3 with high calorific cements (M1: $f_{cm}=14.42$ MPa, M3: $f_{cm}=9.35$ MPa), at the moment of reaching the maximum of the function dQ/dt , is higher than in non-reinforced samples (M1: $f_{cm}=9.78$ MPa, M3: $f_{cm}=8.03$ MPa), but reaches its peak after a longer time. The compressive strength of samples without rebar M2 with low calorific cement ($f_{cm}=3.75$ MPa), at the moment of the maximum of the function dQ/dt is insignificantly lower than that of the reinforced sample ($f_{cm}=4.65$ MPa). It should be noticed that the maximum of the function W , occurs at very high internal temperatures ($50-70^{\circ}\text{C}$), for which strength growth is rapid. In this situation each hour has a significant impact on the strength development. This is presented in Figure 10, where the value of the function increases quickly between the 12th and 24th hour. It is especially visible for concrete M1.

Based on the presented research, it can be stated that rebar protruding from the element (made with high calorific cements) increases the safety of the structure by transferring heat to the outside. The structure reaches higher strength at the moment of thermal impact.

4. CONCLUSION

Based on the results obtained, three groups of conclusion was established:

1) Conclusions related to heat of hydration:

- Higher temperature increase due to hydration is visible in non-reinforced samples (51.8°C for M1, 32.5°C for M2 and 40.8°C for M3) and depend on the calorific value of cement which is used in mixture.
- A high amount of protruding rebar in element samples affects on internal temperature and amount of generation heat in concrete. Differences between temperature of reinforced and non-reinforced samples range from 6.9°C (M3) to 14.0°C (M1) and depended on the calorific value of the cement which is used in mixture.
- Maximum temperature was reached faster in reinforced samples.

2) Conclusions related to comparison of compressive strength of specimen with protruding rebars and without protruding rebar:

- The difference between compressive strength of reinforcement and non-reinforcement specimens for mixes M1 and M3 (M1 – with cement CEM I 52.R, M2

– with cement CEM I 42.5R) is very high for early age concrete (about 5 – 15 %) and stabilizes after 48 hours in level about 3 – 5%.

- For mix M3 (with cement CEM III/A 42.5N) difference between reinforcement and non-reinforcement specimen is about 3-5 % during all maturing period.

3) Conclusions related to comparison of velocity of heat of hydration (dQ/dt) and compressive strength of concrete:

- In mixes M1 and M3, the shift of the maximum of dQ/dt function is about 2h to 3h (maximum of dQ/dt function is theoretically period that can occurs the biggest thermal-shrinkage stresses). The maximum dQ/dt function occurs later in the sample with protruding rebar, so the biggest thermal-shrinkage stresses occurs, when the compressive strength of concrete is 15-50% higher than for the specimen without protruding rebar. The additional temperature gradient for the specimen with protruding rebar is lower.

- In mix M2 (CEM III/A 42.5N) the shift of the maximum dQ/dt function is about 1h. In this case the increase of the compressive strength of concrete is about 25%.

- The presented analysis proves that the protruding rebars is particularly effective for reduce the heat of hydration for the mixes with high calorific cement. For low calorific cements, the efficiency of heat removal by reinforcement is much lower.

To sum up the tests and analyses performed show that protruded rebar can influence of reduction of the internal temperature of hardening concrete in structure. This phenomenon can be included in the risk assessment of possible damage caused by thermal stresses in mass elements with a high degree of reinforcement.

Increases the safety of structures, allowing reaching higher strength before the critical moment, especially in elements made with high calorific cements.

Rebar protruding from elements affects on reduction the temperature gradients and decreases the generated hardening heat. This analysis demonstrate that fear concerning the exceeding of thermal-shrinkage stress in a analysed type of structure is unreasonable.

REFERENCES

1. Z. Bofang, "Thermal Stresses and Temperature Control of Mass Concrete ", Butterworth-Heinemann, Oxford, 2014.
2. Chu, Y. Lee, M.N. Amin, B.-S. Jang, J.-K. Kim, "Application of a thermal stress device for the prediction of stresses due to hydration heat in mass concrete structure ", *Construction and Building Materials* 45: 192–198, 2013.
3. M. Kaszynska, "Mechanical properties of HPC and SCC cured in mass structures ", *Bridge Maintenance, Safety and Management, IABMAS'06, Third International Conference, Porto, Portugal, 2006*.
4. E. Rastrup, "Heat of Hydration in Concrete ", *Magazine of Concrete Research* Vol. 6, No. 17: 79–92 ,1954.
5. B. Chmielewska, A. Garbacz, G. Adamczewski, B. Rymysza, "Thermal Actions on the Materials During Deck and Pavement Construction", *Archives of Civil Engineering* 64: 101-118, 2018.
6. B. Klemczak, A. Knoppik-Wróbel, "Comparison of Analytical Methods for Estimation of Early-Age Thermal-Shrinkage Stresses in RC Walls", *Archives of Civil Engineering* 59: 97-117, 2013.
7. M. Knauff, B. Grzeszykowski, A. Golubińska, "Minimum Reinforcement for Crack Width Control in RC Tensile Elements", *Archives of Civil Engineering* 65: 111-128, 2019.
8. P.G. Kossakowski, J. Ślusarczyk, "A Case Study of Pre-Service Cracks in the Concrete Decks of a Two-Level Basement Car Park", *Archives of Civil Engineering* 63: 79-97, 2017.
9. J.M. Nixon, A.K. Schindler, R.W. Barnes, S.A. Wade, "Evaluation of the maturity method to estimate concrete strength in field applications: Research Report ", *Highway Research Center and Department of Civil Engineering at Auburn University, 2008*.
10. M. Sofi, P.A. Mendis, D. Baweja, "Estimating early-age in situ strength development of concrete slabs", *Construction and Building Materials* 29: 659–666, 2012.
11. H. Nassif, Suksawang N., "Effect of curing methods on durability of high-performance concrete", *Transportation Research Record* 1798: 31–38, 2002.
12. Azenha M., Faria R., Ferreira D., "Identification of early-age concrete temperatures and strains: Monitoring and numerical simulation", *Cement and Concrete Composites* 31 (6): 369–378, 2009.
13. B. Matthieu, B. Farid, T. Jean-Michel, N. Georges, "Analysis of semi-adiabatic tests for the prediction of early-age behavior of massive concrete structures ", *Cement and Concrete Composites* 34 (5): 634–641, 2012.
14. B. Klemczak, A. Knoppik-Wróbel, "Reinforced concrete tank walls and bridge abutments: Early-age behaviour, analytic approaches and numerical models ", *Engineering Structures* 84: 233–251, 2015.
15. E. M. Fairbairn, M. M. Silvano, R. D. T. Filho, J. S. Alves, N. F. Ebecken, "Optimization of mass concrete construction using genetic algorithms ", *Computers & Structures* 82 (2–3): 281–299, 2004.
16. P.J.M. Bartos, "Self-compacting Concrete in Bridge Construction. Guide for design and construction. Concrete Bridge Development Group Technical Guide 7 ", *Concrete Bridge Development Group, Camberley (UK), 2005*.
17. J. Biliszczuk, J. Onysyk, W. Barcik, P. Prabucki, M. Sulkowski, J. Szczepański, R. Toczkiwicz, M. Tomiczek, A. Tukendorf, K. Tukendorf, A. Ast, "Redzinski bridge in the motorway ring road of Wrocław (in Polish)", *Inżyniera i Budownictwo* 2(68): 63–68 ,2012.
18. American Concrete Institute, "Cement and Concrete Terminology ", Farmington Hills, Mich., 2000.
19. J. Gaida, M. Vangeem, "Controlling Temperatures in Mass Concrete: Understanding mass concrete is the key to controlling temperatures and ultimately saving time, effort, and money", *Concrete International* 2002 (January): 59–62 ,2002.
20. H. Ju-Hyung, s.J. Youn, C. Yun-gu, "Thermal crack control in mass concrete structure using an automated curing system", *Automation in Construction* 45: 16–24 ,2014.
21. L. Xinghong, Z. Chao, C. Xiaolin, Z. Wei, C. Yonggang, D. Yin, "Precise simulation analysis of the thermal field in mass concrete with a pipe water cooling system", *Applied Thermal Engineering* 78: 449–459 ,2015.
22. W. R. L. da Silva, V. Šmilauer, P. Štemberk, "Upscaling semi-adiabatic measurements for simulating temperature evolution of mass concrete structures", *Materials and Structures (Valume* 48, Issue 4): 1031–1041, 2013.
23. B. H. Nagaratnam, M. E. Rahman, A. B. Mrasa, M. A. Mannan, S. O. Lame, "Workability and heat of hydration of self-compacting concreteincorporating agro-industrial waste", *Journal of Cleaner Production* 112: 882–894, 2016.
24. A.S.M. Abdul Awal, I.A. Shehu, "Evaluation of heat of hydration of concrete containing high volume palm oil fuel ash", *Fuel* 105: 728–731, 2013.
25. M.R. Jones, A. McCarthy, "Heat of hydration in foamed concrete: Effect of mix constituents and plastic density", *Cement and Concrete Research* 36 (6): 1032–1041 ,2006.
26. EN 197-1:2000 Cement. Composition, specifications and conformity criteria for common cements.
27. EN 1992-1-1: Eurocode 2: Design of concrete structures - Part 1-1: General rules and rules for buildings.
28. EN 10080: Steel for the reinforcement of concrete.

29. EN 206: 2016. Concrete Specification, performance, production and conformity.
30. EN 12350-8:2010. Testing fresh concrete. Self-compacting concrete. Slump-flow test.
31. N.J. Carino, H.S. Lew, "The Maturity Method: From Theory to Application", Proceedings of the 2001 Structures Congress & Exposition: 1–19 ,2001.
32. A. G. Brooks, A.K. Schindler, R. W. Barnes, "Maturity Method Evaluated for Various Cementitious Materials", Journal of Materials in Civil Engineering 19 (12): 1017–1025 ,2007.
33. T.A. Yikici, H.L. Chen, "Use of maturity method to estimate compressive strength of mass concrete", Construction and Building Materials 95: 802–812 ,2015.
34. Y. Lin, H.-L. Chen, "Thermal analysis and adiabatic calorimetry for early-age concrete members Part 2", Journal of Thermal Analysis and Calorimetry 124 (1): 227–239 ,2016.
35. Y. Lin, H.-L. Chen, "Thermal analysis and adiabatic calorimetry for early-age concrete members Part 1", Journal of Thermal Analysis and Calorimetry 122 (2): 937–945 ,2015.
36. M. Soutsos, A. Hatzitheodorou, J. Kwasny, F. Kanavaris, "Effect of in situ temperature on the early age strength development of concretes with supplementary cementitious materials", Construction and Building Materials 103: 105–116 ,2016.
37. S.A. Wade, A.K. Schindler, R.W. Barnes, J.M. Nixon (Eds.), "Maturity Method Report No. 1", Highway Research Center and Department of Civil Engineering at Auburn University, 2006.

LIST OF FIGURES AND TABLES:

Fig. 1. Reinforced concrete sample (with protruding rebar) – cross section (all dimensions are in cm)

Rys. 1. Próbką betonowa z wystającym zbrojeniem – przekrój (wymiarów podano w cm)

Fig. 2. Location of the measurement points inside sample (all dimensions are in cm)

Rys. 2. Lokalizacja punktów pomiarów wewnątrz próbki (wymiarów podano w cm)

Fig. 3. Samples after tests

Rys. 3. Próbkę po badaniach

Fig. 4. Schematic diagram of the test stand under semi-adiabatic conditions

Rys. 4. Schemat stanowiska badawczego dla testów semi-adiabaticznych

Fig. 5. Results of the temperature measurement in concrete M1

Rys. 5. Wynika pomiaru temperatur w betonie M1

Fig. 6. Results of the temperature measurement in concrete M2

Rys. 6. Wynika pomiaru temperatur w betonie M2

Fig. 7. Results of the temperature measurement in concrete M3

Rys. 7. Wynika pomiaru temperatur w betonie M3

Fig. 8. Temperature inside concrete samples (point 1)

Rys. 8. Temperatura wewnątrz próbek betonowych (punkt 1)

Fig. 9. Compressive strength of concrete under isothermal and adiabatic conditions for concretes M1, M2 and M3

Rys. 9. Wytrzymałość betonów M1, M2 oraz M3 na ściskanie w warunkach izotermicznych i adiabaticznych

Fig. 10. Compressive strength of concrete M1, M2, M3 at the maximum of dQ/dt

Rys. 10. Wytrzymałość betonu M1, M2, M3 na ściskanie w momencie maksimum funkcji dQ/dt

Table 1. Concrete mix composition

Tab. 1. Składów mieszanek betonowych

Table 2. Composition of cements used in experiments

Tab. 2 Skład chemiczny cementów użytych w badaniach

Table 3. Composition of fly ash used in experiments

Tab. 3. Skład chemiczny popiołu lotnego użytego w badaniach

Table 4. Workability properties of concrete

Tab. 4. Właściwości reologiczne betonu

Table 5. Maximum temperature in concrete samples, T_{\max} [°C]

Tab. 5. Maksymalna temperatura w próbkach betonowych, T_{\max} [°C]

Table 6. Time after concrete reached maximum temperature [hours]

Tab. 6. Czas, po którym beton osiągnął maksymalną temperaturę [h]

Table 7. Self-heating of concretes

Tab. 7. Przyrost temperatury betonu podczas badania

Table 8. Maximum temperature differences between reinforced and non-reinforced concrete

Tab. 8. Maksymalna różnica temperatur między próbką zbrojoną i niezbrojoną

Table 9. Compressive strength of concrete [MPa] under laboratory conditions (20°C)

Tab. 9. Wytrzymałość betonu na ściskanie [MPa] w temperaturze laboratoryjnej (20°C)

Table 10. Compressive strength of concrete [MPa] under semi - adiabatic conditions (point C1)

Tab. 10. Wytrzymałość betonu na ściskanie [MPa] w warunkach semi-adaibatycznych (punkt C1)

Table 11. Compressive strength of concrete [MPa] under semi-adiabatic conditions (point R1)

Tab. 11. Wytrzymałość betonu na ściskanie [MPa] w warunkach semi-adaibatycznych (punkt R1)

Table 12. The comparison between compressive strength of concretes cured in condition from point C1 and point R1

Tab. 12. Porównanie wytrzymałości na ściskania betonów dojrzewających w warunkach punktu C1 oraz punktu R1

Table 13. Comparison of the compressive strength of concrete M1, M2, M3 at the maximum of dQ/dt

Tab. 13. Porównanie wytrzymałości betonów M1, M2, M3 na ściskanie w momencie maksimum funkcji dQ/dt

WPLYW WYSTAJĄCEGO Z ELEMENTU BETONOWEGO ZBROJENIA NA ROZWÓJ TEMPERATURY I WYTRZYMAŁOŚĆ NA ŚCISKANIE BETONU W CZASIE JEGO DOJRZEWANIA

Keywords: wytrzymałość na ściskanie; temperatura dojrzewania; beton samozagęszczalny; wystające pręty zbrojeniowe; konstrukcje masywne

SUMMARY:

W artykule przeanalizowano wpływ wystającego z elementu betonowego zbrojenia na rozwój temperatury i wytrzymałości betonu na ściskanie podczas wznoszenia konstrukcji. Wystające zbrojenie może symulować warunki panujące podczas betonowania takich elementów jak przyczółki mostowe czy pylony.

Celem badań było ustalenie zależności między ilością generowanego ciepła i wczesną wytrzymałością na ściskanie dla samozagęszczalnych betonów dojrzewających w konstrukcjach masywnych. Wyniki badań mogą być wykorzystane przy opracowaniu technologii betonowania w budownictwie mostowym.

W ramach badań wykonano w zaizolowanych termicznie systemowych szalunkach próbki o wymiarach 50 cm x 50 cm x 50 cm z wystającym z konstrukcji zbrojeniem (symulujące element podczas przerwy roboczej) oraz element referencyjny bez zbrojenia. Zastosowane pręty zbrojeniowe miały średnicę 2 cm i długość 80 cm. Jeden koniec pręta znajdował się 20 cm od dna szalunku i wystawał 33 cm ponad jego górną izolację termiczną. W próbce znajdowało się 36 równomiernie rozłożonych prętów zbrojeniowych, co daje stopień zbrojenia równy 4.5%.

Temperatura była mierzona podczas dojrzewania betonu za pomocą termopary typu T osadzonej w betonie. Termopary były przymocowane do zbrojenia. Natomiast w próbce niezbrojonej termopary były umieszczone w betonie za pomocą specjalnego zaizolowanego pręta. Temperatura była mierzona przez 7 dni w 5 minutowym interwale czasowym, za pomocą aparatury ConReg 706. Próbka zbrojona i niezbrojona podczas badania były wykonane w tym samym czasie. Termopary były umieszczone w szalunku i podłączone do aparatury pomiarowej przed rozpoczęciem badania. Temperatura wewnątrz próbki była mierzona w trzech punktach: w środku próbki (punkt 1), 5 cm od bocznej krawędzi (punkt 2) oraz 5 cm od górnej krawędzi (punkt 3).

W badaniach użyto 3 cementów: cementów portlandzkich CEM I 52.5R i CEM I 42.5R oraz cementu hutniczego CEM III/A 42N. Składy wszystkich mieszanek były takie same. Zgodnie z oczekiwaniami najwyższa temperatura została zarejestrowana w betonie z cementem CEM I 52.5R, następnie w betonie z cementem CEM I 42.5R, natomiast najniższa w betonie z cementem CEM III/A 42.5N. W próbce niezbrojonej najwyższą temperaturę zaobserwowano po 27 godzinach w betonie z CEM I 52.5R, po 33 godzinach w betonie z CEM I 42.5R oraz po 48 godzinach w betonie z CEM III/A 42N. Najwyższa temperatura w próbkach ze zbrojeniem została zarejestrowana w betonie M1 (CEM I 52.5R) po 24 h, w betonie M2 (CEM III/A 42.5N) po 37 godzinach oraz w betonie M3 (CEM I 42.5R) po 21 godzinach. Ten efekt, przesunięcia momentu, w którym wystąpiła najwyższa temperatura jest spowodowany szybszą ucieczką ciepła przez pręty zbrojeniowe. Różnica między czasem w którym próbka zbrojona i próbka niezbrojona uzyskiwała maksymalną temperaturę jest w przedziale od 3 do 12 godzin.

Zarejestrowane temperatury w zbrojonych i niezbrojonych próbkach betonowych posłużyły do obliczenia ilości (Q) i kinetyki (dQ/dt) wydzielania ciepła a następnie do sterowania temperatury w komorze klimatycznej, w której przechowywane były próbki do badań wytrzymałości betonu na ściskanie.

Wytrzymałość na ściskanie betonu M1 i M3 dojrzewającego w temperaturze zarejestrowanej w próbkach z wystającym zbrojeniem wyniosła odpowiednio (M1: $f_{cm} = 14.42$ MPa, M3: $f_{cm} = 9.35$ MPa), i w momencie wystąpienia maksimum funkcji dQ/dt jest wyższa niż wytrzymałość betonu dojrzewającego w próbce niezbrojonej (M1: $f_{cm} = 9.78$ MPa, M3: $f_{cm} = 8.03$ MPa). Wytrzymałość na ściskanie betonu w próbce z cementem hutniczym ($f_{cm} = 3.75$ MPa) w momencie wystąpienia maksimum funkcji dQ/dt jest znacząco niższa niż dla próbki zbrojonej ($f_{cm} = 4.65$ MPa). Należy zaznaczyć, że maksimum funkcji dQ/dt występuje, gdy jest bardzo wysoka temperatura wewnątrz próbki (50-70°C) dla której wzrost wytrzymałości jest bardzo szybki. W tym przypadku każda godzina ma znaczący wpływ na rozwój wytrzymałości.

Wnioski z badań podzielono na trzy grupy:

1) Wnioski związane z ciepłem twardnienia betonu:

- W próbkach niezbrojonych przyrost temperatury jest zdecydowanie wyższy niż w próbkach zbrojonych (51.8°C dla M1, 32.5°C dla M2 i 40.8°C dla M3).

- Różnica temperatury między próbka zbrojoną i niezbrojoną (rozpatrując ten sam punkt) jest w przedziale od 6.9°C (M3) do 14.0°C (M1) i zależy od kaloryczności użytego cementu.

- Próbki z wystającym zbrojeniem szybciej uzyskiwały maksymalną temperaturę.

2) Wnioski z porównania rozwoju wytrzymałości na ściskanie betonu w próbce zbrojonej i niezbrojonej:

- Różnica między wytrzymałością na ściskanie betonu M1 i M3 (mieszanki z cementami CEM I 52.5 R oraz CEM I 42.5R) dojrzewającego w próbce zbrojonej i niezbrojonej jest bardzo duża w pierwszym okresie dojrzewania betonu (około 5 – 15%) i stabilizuje się po 48 godzinach w granicy 3 – 5%.

- W przypadku betonu M3 (na cementie CEM III/A 42.5N) różnica wytrzymałości na ściskanie betonu w próbce zbrojonej i niezbrojonej jest w granicach 3-5% przez cały okres dojrzewania.

3) Wnioski związane z porównaniem szybkości wydzielania ciepła a wzrostem wytrzymałości betonu na ściskanie:

- W betonach M1 i M3 przesunięcie maksimum funkcji dQ/dt , wynosi około 3h i 2h i występuje później w próbce z wystającym zbrojeniem, więc w momencie wystąpienia największych naprężeń termiczno-skurczowych wytrzymałość na ściskanie tego betonu jest o 15 – 50 % większa niż dla próbki bez wystającego zbrojenia, dodatkowa gradient temperatury dla próbki zbrojonej jest niższy.

- W betonie M2 (na cementie CEM III/A 42.5N) przesunięcie maksimum funkcji dQ/dt jest o około 1h, a zwiększenie wytrzymałości betonu na ściskanie w tym przypadku to około 25 %.

- Przedstawiona analiza dowodzi, że wystające zbrojenie jest szczególnie skuteczne w obniżeniu ciepła twardnienia wtedy gdy mieszanka zawiera wysokokaloryczny cement. Dla cementów niskokalorycznych skuteczność odprowadzenia ciepła przez zbrojenie jest zdecydowanie mniejsza.

Badania i analizy pokazują, że pręty wystające z masywnego elementu betonowego wpływają na redukcję wewnętrznej temperatury twardniejącego betonu w konstrukcji. To zjawisku powinno być wzięte pod uwagę podczas analizy powstawania rys termiczno-skurczowych w masywnych elementach betonowych z wysokim stopniem zbrojenia.

